Spontaneous and explicit parity-time-symmetry breaking in drift-wave instabilities

Hong Qin,[1,*] Yichen Fu,[1] Alexander S. Glasser,[1] and Asher Yahalom[2,1]
[1]*Plasma Physics Laboratory, Princeton University, Princeton, New Jersey 08543, USA*
[2]*Ariel University, Ariel 40700*

(Received 25 October 2020; revised 6 July 2021; accepted 7 July 2021; published 28 July 2021)

A method of parity-time- (PT) symmetry analysis is introduced to study the high-dimensional, complicated parameter space of drift-wave instabilities. We show that spontaneous PT-symmetry breaking leads to the ion temperature gradient instability of drift waves, and the collisional instability is the result of explicit PT-symmetry breaking. A new unstable drift wave induced by finite collisionality is identified. It is also found that gradients of ion temperature and density can destabilize the ion cyclotron waves when PT symmetry is explicitly broken by a finite collisionality.

DOI: 10.1103/PhysRevE.104.015215

Drift-wave instability driven by density gradient is an important research topic for plasma physics and magnetic fusion [1–6]. The turbulence transport in tokamaks starts from the seed of drift waves destabilized by various effects that naturally exist in the devices. The drift-wave and associated instabilities in tokamaks typically depend on seven or eight dimensionless parameters, including the scale lengths of the ions and electrons, as well as impurity levels and collisionality. The complicated parameter dependency of the drift wave results in many different paths to instabilities, which have been extensively studied in the past. Well-known examples include the ion temperature gradient (ITG) mode, or the η_i mode [7,8], the universal mode driven by nonadiabatic electron response [9,10], the electron temperature gradient mode [11–13], and the collisional drift instability [14–16], just to name a few. The neoclassical effect in the toroidal geometry can also destabilize the drift wave as in the trapped particle modes [17,18]. Because of the complexity in parameter space and destabilization mechanisms, recent studies of drift-wave instabilities rely on numerical simulations [19] using the gyrokinetic [8,11,13,20–22] or gyrofluid methods [23–25].

In the present study, we introduce a new perspective to understand the mechanism of drift-wave instabilities using the tool of parity-time- (PT) symmetry analysis. PT symmetry is a concept in non-Hermitian quantum physics [26–28] introduced by Bender and collaborators [29–36]. It has found a wide range of applications in many branches of physics. It was recently applied to study instabilities in continuous media, such as the classical Kelvin-Helmholtz instability and the Rayleigh-Taylor instability [37,38]. Here, using a two-fluid model in a slab geometry, we show that drift-wave instabilities in magnetized plasmas can be divided into two classes that are induced by spontaneous PT-symmetry breaking and explicit PT-symmetry breaking, respectively. This finding provides a new tool to navigate the complex parameter space [19] of the drift-wave instabilities.

Spontaneous PT-symmetry breaking happens in conservative systems via Krein resonances [36,39–41] between two eigenmodes with opposite signs of actions. Explicit PT-symmetry breaking occurs in nonconservative systems, and it is often associated with dissipative instabilities [42]. Because the spectrum of a PT-symmetric system must be symmetric with respect to the real axis, instabilities arise when and only when an eigenmode violates PT symmetry, i.e., PT symmetry is spontaneously broken. As a consequence, spontaneous PT-symmetry breaking usually has a finite threshold in the parameter space corresponding to the Krein resonance. If a physical effect is introduced into the system such that it does not admit PT symmetry anymore, we say that PT symmetry is explicitly broken. For such a system, the constraints on the distribution of the spectrum are removed, and instabilities are easier to trigger. When explicit PT-symmetry breaking destabilizes the system, in most cases, there is no finite threshold for the onset of instabilities.

We will use the example of the ITG instability and the collisional instability to demonstrate the physics of spontaneous and explicit PT-symmetry breaking in drift waves, respectively. In particular, we show that the governing equation of the ITG mode is PT symmetric, and spontaneous PT-symmetry breaking leads to the ITG instability. The finite threshold of the ITG mode corresponds to the Krein resonance for spontaneous PT-symmetry breaking. On the other hand, the collisions between electrons and ions explicitly breaks PT symmetry, and there is no threshold for the collisional instability. When the gradient of temperature or density exists, any small collisionality will induce a growth rate for the drift waves. A finite collisionality also induces a new unstable low-frequency drift wave, which will be temporarily called collision-induced drift wave for lacking of a better terminology.

In addition, within the model adopted, we found that temperature gradient and density gradient are destabilizing for the electrostatic cyclotron waves as well. Because of the strong constraint of PT symmetry, the threshold for instability is too high for the parameters of practical interest. However,

*hongqin@princeton.edu

when PT symmetry is explicitly broken by a small but finite collisionality, the gradients of ion temperature and density can drive the electrostatic cyclotron waves unstable without any threshold.

We first demonstrate the mechanism of spontaneous PT-symmetry breaking for the local ITG mode in a slab geometry using a conservative two-fluid model. For each species, the governing equations are

$$\frac{\partial n_j}{\partial t} + \nabla \cdot (n_j \boldsymbol{u}_j) = 0, \tag{1}$$

$$m_j n_j \left(\frac{\partial \boldsymbol{u}_j}{\partial t} + \boldsymbol{u} \cdot \nabla \boldsymbol{u} \right) = Z_j n_j e \left(\boldsymbol{E} + \frac{\boldsymbol{v} \times \boldsymbol{B}}{c} \right) - \nabla p_j, \tag{2}$$

$$\frac{d}{dt} \left[\frac{p_j}{(m_j n_j)^{\gamma_j}} \right] = 0, \tag{3}$$

where Z_j is charge number and γ_j is the polytropic index for the jth species.

The equilibrium consists of a constant magnetic field in the z direction, $\boldsymbol{B} = B\boldsymbol{e}_z$, and inhomogeneous density $n_{j0}(x)$ and pressure $p_{j0}(x) = n_{j0}(x)T_{j0}(x)$ of electrons and ions. The gradients of densities and pressures are in the x direction. Quasineutrality condition requires $Z_i n_{i0} = n_{e0}$. Because the equilibrium is inhomogeneous, particles flow in the diamagnetic direction. We assume that an equilibrium electrostatic field in the x direction is established such that only electrons flow in the diamagnetic direction, i.e.,

$$\boldsymbol{u}_{i0} = 0, \tag{4}$$

$$\boldsymbol{u}_{e0} = -\left[\frac{cE_0(x)}{B} + \frac{c}{eBn_{e0}} \frac{dp_{e0}(x)}{dx} \right] \boldsymbol{e}_y, \tag{5}$$

$$\boldsymbol{E}_0(x) = E_0(x)\boldsymbol{e}_x = \frac{1}{Z_i n_{i0}(x) e} \frac{dp_{i0}(x)}{dx} \boldsymbol{e}_x . \tag{6}$$

For linear electrostatic perturbation, we consider a local mode in the form of $\exp(ik_y y + ik_z z - i\omega t)$. For the ITG mode, electron density perturbation can be approximated by the adiabatic response (see Appendix),

$$Z_i n_{i1}(x) = n_{e1}(x) = \frac{e n_{e0} \phi_1}{m_e T_{e0}}, \tag{7}$$

where the first equal sign is due to the quasineutrality condition. Ions' response is governed by the linearized system of Eqs. (1)–(3),

$$-i\omega n_{i1} = -ik_z n_{i0} u_{iz1} - ik_y n_{i0} u_{iy1} - u_{ix1} \frac{dn_{i0}}{dx}, \tag{8}$$

$$-i\omega u_{ix1} = \frac{Z_i e u_{iy1} B_0}{c m_i} + \frac{1}{m_i n_{i0}^2} \frac{dp_0}{dx} n_{i1}, \tag{9}$$

$$-i\omega u_{iy1} = -\frac{ik_y Z_i e \phi_1}{m_i} - \frac{Z_i e u_{ix1} B_0}{c m_i} - \frac{ik_y p_{i1}}{m_i n_{i0}}, \tag{10}$$

$$-i\omega u_{iz1} = -\frac{ik_z Z_i e \phi_1}{m_i} - \frac{ik_z p_{i1}}{m_i n_{i0}}, \tag{11}$$

$$-i\omega p_{i1} = -u_{ix1} \frac{dp_{i0}}{dx} - \gamma_i p_{i0} (ik_y u_{iy1} + ik_z u_{iz1}) . \tag{12}$$

We choose the following normalization and dimensionless parameters:

$$\bar{t} = t\Omega_i,\ \bar{x} = \frac{x}{a},\ \bar{k}_{y,z} = k_{y,z} a,\ \bar{k}_n = \frac{1}{n_{i0}} \frac{dn_{i0}}{dx} a\ , \tag{13}$$

$$\bar{u}_{ix1,iy1,iz1} = \frac{u_{ix1,iy1,iz1}}{a\Omega_i},\ \bar{v}_{\rm thi}^2 \equiv \frac{T_{i0}}{m_i a^2 \Omega_i^2},\ \bar{v}_s^2 \equiv \frac{Z_i T_{e0}}{m_i a^2 \Omega_i^2},$$

$$\bar{p}_{i1} = \frac{p_{i1}}{n_{i0} m_i \Omega_i^2 a^2}, \tag{14}$$

$$\bar{\omega}_T^\dagger \equiv \frac{1}{m_i a \Omega_i^2} \frac{dT_{i0}}{dx},\ \bar{\omega}_p^\dagger \equiv \frac{1}{m_i n_{i0} a \Omega_i^2} \frac{dp_{i0}}{dx} = \bar{k}_n \bar{v}_{\rm thi}^2 + \bar{\omega}_T^\dagger. \tag{15}$$

Here $\Omega_i = Z_i eB/m_i c$ is the ion gyrofrequency, and a is the typical scale length of the system, which can be chosen to be the minor radius of a tokamak. The dimensionless parameter $\bar{k}_n$ measures the density gradient, and $\bar{\omega}_T^\dagger$ measures the ion temperature gradient. Substituting Eq. (7), we cast the linear system Eqs. (8)–(12) into the form of Schrödinger's equation,

$$H\psi = \omega\psi, \tag{16}$$

$$H = \begin{pmatrix} 0 & -ik_n & k_y & k_z & 0 \\ i\omega_p^\dagger & 0 & i & 0 & 0 \\ v_s^2 k_y & -i & 0 & 0 & k_y \\ v_s^2 k_z & 0 & 0 & 0 & k_z \\ 0 & i\omega_p^\dagger & \gamma_i v_{\rm thi}^2 k_y & \gamma_i v_{\rm thi}^2 k_z & 0 \end{pmatrix}, \tag{17}$$

$$\psi = (n_{i1}, u_{ix1}, u_{iy1}, u_{iz1}, p_{i1})^T . \tag{18}$$

All quantities in Eqs. (16)–(18) are normalized and dimensionless. For easy notation, the over bars for normalized quantities have been dropped. This convention will be adopted hereafter unless explicitly stated otherwise.

The spectrum of the system is determined by the characteristic polynomial of H,

$$D(\omega) = -\omega^5 + \alpha\omega^3 + \beta\omega^2 + \xi\omega = 0, \tag{19}$$

$$\alpha \equiv 1 + k_n^2 v_{\rm thi}^2 + \left(k_y^2 + k_z^2\right)\left(v_s^2 + \gamma_i v_{\rm thi}^2\right) + k_n \omega_T^\dagger, \tag{20}$$

$$\beta \equiv k_y \left[2\omega_T^\dagger + k_n \left(2v_{\rm thi}^2 + v_s^2 \right) \right], \tag{21}$$

$$\xi \equiv -k_n^2 \left(k_y^2 + k_z^2\right) v_{\rm thi}^4 (\gamma_i - 1) - k_z^2 \left(v_s^2 + \gamma_i v_{\rm thi}^2\right) \tag{22}$$

$$- k_n \left(k_y^2 + k_z^2\right) v_{\rm thi}^2 (\gamma_i - 2) \omega_T^\dagger + \left(k_y^2 + k_z^2\right) \omega_T^{\dagger 2}. \tag{23}$$

The spectrum are determined by seven dimensionless parameters and consist of two high-frequency ion cyclotron modes and two low-frequency drift modes. The zero frequency mode is not physically significant unless other effects, such as the collisions, are considered. We will come back to this mode later.

In a homogeneous equilibrium, $k_n = 0$, $\omega_T^\dagger = 0$, and we can set $k_z = 0$ to observe that the dispersion relation for the two high-frequency waves reduces to (in un-normalized variables)

$$\omega^2 = \Omega_i^2 + k_y^2 \left(v_s^2 + \gamma_i v_{\rm thi}^2 \right), \tag{24}$$

which is the dispersion relation of the electrostatic ion cyclotron waves in a homogeneous, magnetized plasma. The dispersion relation for the two drift waves reduce to $\omega = 0$, since the equilibrium is homogeneous.

We would like to know when the drift waves, and the electrostatic ion cyclotron waves, will become unstable. Because the parameter space is seven dimensional, the boundary between stability and instability in the parameter space

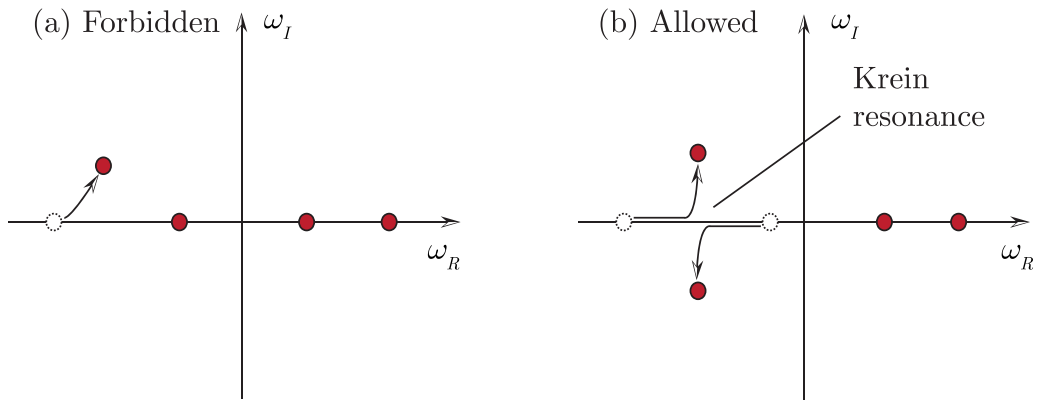

FIG. 1. Forbidden path (a) and allowed path (b) for instabilities as system parameters varying for a PT-symmetric system, illustrated for systems with four eigenmodes. A PT-symmetric system can be destabilized only by the spontaneous PT-symmetry breaking through the Krein resonance (b).

might be complicated. It turns out that PT-symmetry analysis can help us to understand how the instability is triggered in the parameter space.

Even though Eq. (16) assumes the form of Schrödinger's equation, the Hamiltonian specified by H in Eq. (17) is not Hermitian as in standard quantum mechanics. Otherwise, ω would always be real and the system would be stable. As we show now, H is PT symmetric instead, which allows instabilities.

Note that when the background is homogeneous, $k_n = 0$ and $\omega_T^\dagger = 0$, then H is similar to a Hermitian matrix via a simple rescaling of variables. This is akin to the situation of cold plasma waves in a homogeneous medium [43]. It is the background inhomogeneity that breaks the Hermiticity of the system, and transforms it into a more interesting PT-symmetric system [44].

A non-Hermitian operator H is PT symmetric if H commutes with an PT operator, i.e.,

$$PTH = HPT\,. \tag{25}$$

Here P is a linear parity operator satisfying $P^2 = I$ and T is the complex conjugate operation [31]. We briefly summarize the properties of PT symmetry as follows. The spectrum of a PT-symmetric operator must be symmetric with respect to the real axis, which is a strong constraint on the distribution of the eigenmodes. For a stable system to become unstable under the variation of system parameters, two eigenmodes of the system must resonate first, which is called Krein resonance [36,39–41]. A stable eigenmode is forbidden to move away from the real axis by itself without going through the Krein resonance with another stable mode. This situation is illustrated in Fig. 1. It is also known that only Krein resonances between two stable eigenmodes with opposite signs of actions result in destabilization [36,39–41,45,46]. After resonance between two stable modes with the same sign of actions, the modes remain stable. Furthermore, when the system is stable, any eigenvector ψ admits PT symmetry, i.e., $PT\psi = \lambda\psi$ for some complex number λ. In this case, we say PT symmetry is unbroken. When an eigenmode is destabilized after the Krein resonance, it must also break PT symmetry, i.e., $PT\psi \neq \lambda\psi$ for any complex number λ. This is known as spontaneous PT-symmetry breaking. These eigenmode properties have been identified for applications in plasma physics and beam physics [37,38,45,47–50].

Returning to the Hamiltonian H for the coupled system of drift waves and ion cyclotron waves specified by Eq. (17), we verify that H is indeed PT symmetric for

$$P = \begin{pmatrix} 1 & & & & \\ & -1 & & & \\ & & 1 & & \\ & & & 1 & \\ & & & & 1 \end{pmatrix}. \tag{26}$$

This confirms that the system can only be destabilized by spontaneous PT-symmetry breaking through the Krein resonance. The point where the resonance occurs marks the threshold of the instability. Such a process is displayed in Fig. 2, where the real frequency ω_R and the growth rate ω_I of the four eigenmodes are plotted against $\omega_T^\dagger$ for a typical set of parameters of tokamaks. The range of $\omega_T^\dagger$ is between 10^{-5} and 10^{-4}. Other dimensionless parameters are $v_{\rm thi}^2 = 4\times10^{-6}$, $v_s^2 = 4\times10^{-6}$, $k_n = 5$, $k_y = 400$, $k_z = 1$, and $\gamma_i = 1$. It is clear that the spectrum is symmetric with respect to the real axis as required by PT symmetry. The spontaneous PT-symmetry breaking for the low-frequency drift waves starts at $\omega_T^\dagger = 3.4\times10^{-5}$, where two of stable drift waves resonate, and above this threshold the drift wave is unstable. This is the familiar ITG instability. It can be verified that the signs of actions for the two stable modes are different at the threshold, as required by the mechanism of the Krein resonance. For brevity, the calculation of signs of actions for eigenmodes [45] are omitted here.

PT-symmetry analysis also reveals certain polarization property of the ITG mode. When the ITG mode is stable, i.e., when PT symmetry is unbroken, the eigenmode preserves PT symmetry,

$$PT\psi = P\psi^* = \lambda\psi\,, \tag{27}$$

where $*$ denote complex conjugate. For the form of P specified in Eq. (26), we can conclude that the relative phase between n_{i1} and u_{ix1} needs to be locked at $\pi/2$ when the ITG mode is stable. When the ITG instability is triggered, this relative phase become undetermined. These characteristics

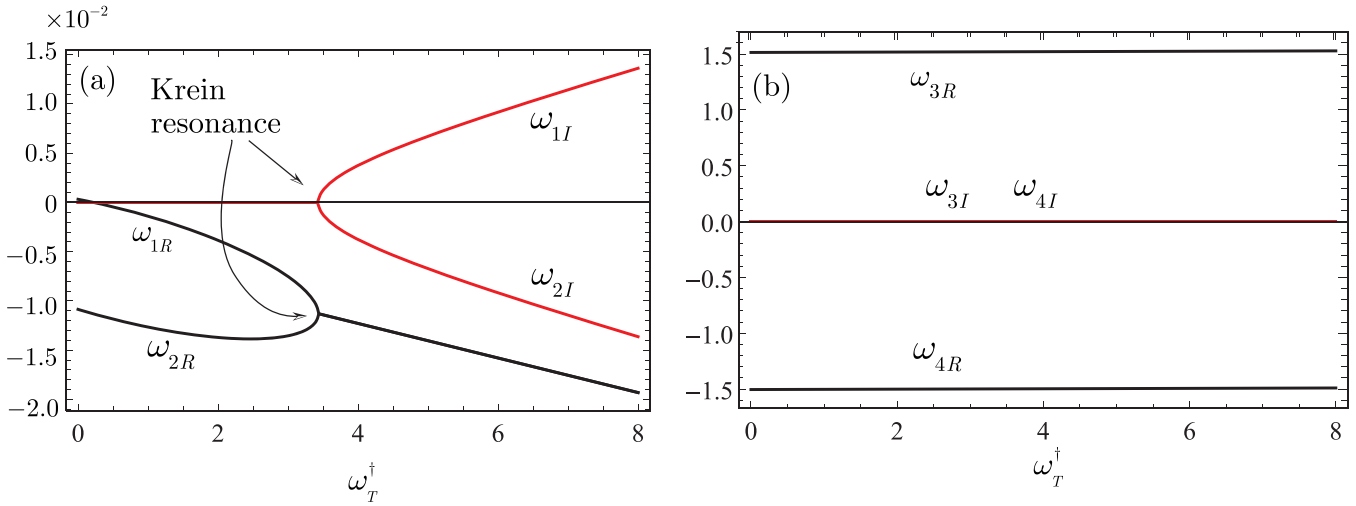

FIG. 2. (a) ITG instability destabilized by spontaneous PT-symmetry breaking through the Krein resonance when the ITG increases. (b) The electrostatic ion cyclotron waves are stable. The gradients of temperature and density are destabilizing factors for the electrostatic ion cyclotron waves. However, the instability threshold imposed by PT symmetry is too high for parameters of practical interest.

might be useful for identifying and validating the stabilization and destabilization processes of the ITG mode in experiments [51,52].

The drift-wave frequency is much smaller than that of the ion cyclotron frequency as shown in Fig. 2. For drift waves, we can neglect the ω^5 term in Eq. (19), and the condition for the ITG instability or spontaneous PT-symmetry breaking becomes

$$\beta^2 \leqslant 4\alpha\xi, \tag{28}$$

where the equal sign holds at the threshold or the Krein resonance point.

In this region of parameter space, the electrostatic ion cyclotron branch is stable without spontaneous PT-symmetry breaking. The gradients of temperature and density are destabilizing factors for the electrostatic ion cyclotron waves. However, for parameters of practical interest, the threshold imposed by PT symmetry is too high for the instability to occur. It turns out that the gradients of ion temperature and density can drive both the electrostatic ion cyclotron modes and the drift waves unstable without threshold, when PT symmetry is explicitly broken by collisions between electrons and ions, which we now investigate.

As mentioned above, explicit PT-symmetry breaking means that the governing equations do not admit a PT symmetry anymore due to some physical effects, which are usually associated with nonconservative effects, such as dissipation. For the drift-wave dynamics studied here, such situations arise when the collisional effect [14–16] or nonadiabatic kinetic response [9,10,17,18] are important. For the model adopted in the present study, if we consider the collision between electrons and ions in the parallel direction, electrons' response is not purely adiabatic anymore, and the relationship between perturbed potential ϕ_1 and $n_{e1} = Z_i n_{i1}$ is (in un-normalized quantities)

$$\phi_1 = \left[\frac{T_{e0}}{e} + i\frac{\nu_{ie}k_y m_i \Delta u_0}{Z_i e k_z^2}(u_{e0} - u_{i0})\right]\frac{n_{i1}}{n_{i0}}, \tag{29}$$

where ν_{ie} is the collision frequency between ions and electrons, and $\Delta u_0 \equiv u_{e0} - u_{i0}$ is difference between the equilibrium flows of electrons and ions specified by Eqs. (4) and (5), respectively. The Hamiltonian of the system is modified as

$$H_\nu = H + \begin{pmatrix} 0 & 0 & 0 & 0 & 0 \\ 0 & 0 & 0 & 0 & 0 \\ \frac{i\nu_{ie}\Delta u_0 k_y^2}{k_z^2} & 0 & 0 & 0 & 0 \\ 0 & 0 & 0 & 0 & 0 \\ 0 & 0 & 0 & 0 & 0 \end{pmatrix}, \tag{30}$$

where ν_{ie} has been normalized by Ω_i and Δu_0 by $a\Omega_i$, following the scheme in Eqs. (13)–(15). The derivation of Eqs. (29) and (30) are given in Appendix.

It can be verified that H_ν is not PT symmetric, i.e., there exists no parity operator P such that $PTH = HTP$. Thus, the constraint on the spectrum associated with PT-symmetric system are removed by the collisions between ions and electrons. An eigenfrequency can move into the complex plane without the necessity of going through the Krein resonance first. The forbidden path for instabilities in Fig. 1(a) is allowed when PT symmetry is explicitly broken. In this sense, the explicit PT-symmetry breaking due to dissipation "loosens up" the dynamics of the system, and makes the system more susceptible to other instability driving factors. This explains why the collision can drive the drift wave unstable, even though it takes energy out of the system as a dissipative effect. In Fig. 3, the destabilization of the drift waves and ion cyclotron waves induced by the finite collisionality is shown. The instabilities have no threshold. A finite collisionality, no matter how small, will lead to a finite growth rate. The dimensionless parameters for this case are $v_{\rm thi}^2 = 2 \times 10^{-6}$, $v_s^2 = 2 \times 10^{-6}$, $\omega_T^\dagger = 10^{-4}$, $k_n = 5$, $k_y = 100$, $k_z = 1$, and $\gamma_i = 1$.

As we see in Fig. 2 for the case without collisions, ion temperature gradient can only destabilize the drift waves above certain threshold and has no effect on the stable ion-cyclotron waves. This can be attributed to the constraints imposed by PT symmetry. But when PT symmetry is broken explicitly by

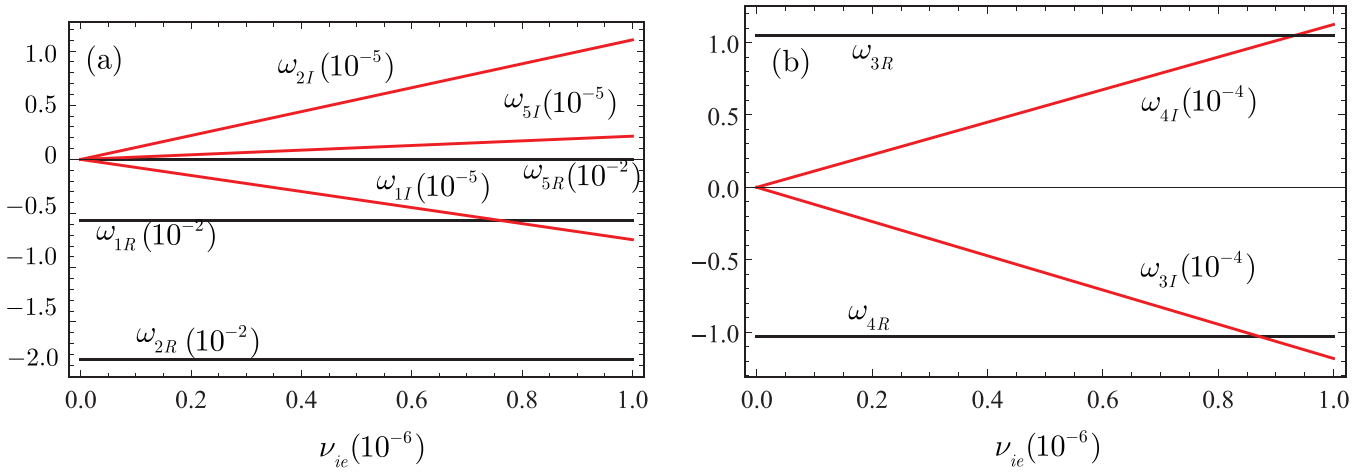

FIG. 3. Drift waves (a) and electrostatic ion cyclotron waves (b) are destabilized by the temperature and density gradients without threshold when PT symmetry is broken explicitly by a small but finite collisionality.

a small but finite collisionality, the temperature and density gradients destabilize both the drift waves and the electrostatic ion cyclotron waves without threshold.

It has been well known that the ITG mode [7,8] has an instability threshold, whereas the collisional drift instability [14–16], the universal mode [9,10], and trapped particle modes [17,18] usually do not. However, the reason for this difference has not been identified in the literature. The analysis from the PT-symmetry perspective provides an answer. The knowledge on the difference between these two types of instability mechanisms is valuable when design laboratory experiments. For the instabilities driven by spontaneous PT-symmetry breaking, such as the ITG mode, the system is structurally stable in the sense that an infinitesimal perturbation or uncertainty on the system parameters will not change the stability property of the system, i.e., a stable system is also stable if the system parameters vary by a small amount. However, this not the case for the instabilities driven by explicit PT-symmetry breaking, e.g., the collisional instability and the universal mode in the context of drift-wave instabilities. Therefore, instabilities triggered by explicit PT-symmetry breaking are relatively more difficult to suppress.

Another noteworthy result is that finite collisionality also induces a new low frequency drift mode which is an almost purely growing mode with an extremely small real frequency. This mode, whose frequency is $\omega_{5R} + i\omega_{5I}$ as in Fig. 3(a), corresponds to the zero frequency mode of the dispersion relation (19) when $\nu_{ie} = 0$. Finite collisionality brings it to life. Let's call it collision-induced drift wave. We are not aware of any previous study of this mode either theoretically or experimentally.

ACKNOWLEDGMENT

This research was supported by the U.S. Department of Energy (DE-AC02-09CH11466).

APPENDIX: NONADIABATIC RESPONSE OF ELECTRONS DUE TO COLLISIONS

In this Appendix, we derive electrons' nonadiabatic response to the perturbed potential when the collisions between electrons and ions are taken into account within the two-fluid model. The derivation is given using un-normalized quantities.

From the fluid equations, the adiabatic electron response can be obtained from the perturbed parallel momentum equation of electrons,

$$eik_z\phi_1 - ik_z T_{e0}\frac{n_{e1}}{n_{e0}} = 0, \tag{A1}$$

where the electron inertial and temperature perturbation have been neglected. To model the nonadiabatic electron response due to electron-ion collisions, we augment Eq. (A1) with a term describing the momentum exchange induced by the collisions,

$$eik_z\phi_1 - ik_z T_{e0}\frac{n_{e1}}{n_{e0}} - m_e\nu_{ei}(u_{e1z} - u_{i1z}) = 0. \tag{A2}$$

Similarly, the perturbed parallel momentum equation for ions (11) is modified to

$$-i\omega u_{iz1} = -\frac{ik_z Z_i e\phi_1}{m_i} - \frac{ik_z p_{i1}}{m_i n_{i0}} - \nu_{ie}(u_{iz1} - u_{ez1}). \tag{A3}$$

Momentum conservation requires that $\nu_{ie} = \nu_{ei}Z_i m_e/m_i$. To obtain a closed expression for the collision term $m_e\nu_{ei}(u_{e1z} - u_{i1z})$, we look at the continuity equation for both species,

$$-i\omega n_{i1} = -ik_y u_{i0}n_{i1} - ik_z n_{i0}u_{i1z} + \frac{ick_y}{B}\frac{dn_{i0}}{dx}\phi_1, \tag{A4}$$

$$-i\omega n_{e1} = -ik_y u_{e0}n_{e1} - ik_z n_{e0}u_{e1z} + \frac{ick_y}{B}\frac{dn_{e0}}{dx}\phi_1, \tag{A5}$$

where the perturbed perpendicular flows for both species have been approximated by the $\boldsymbol{E}\times\boldsymbol{B}$ flow due to ϕ_1. With the quasineutrality condition, Eqs. (A4) and (A5) lead to

$$u_{e1z} - u_{i1z} = -\frac{k_y}{k_z}(u_{e0} - u_{i0})\frac{n_{i1}}{n_{i0}}. \tag{A6}$$

Substituting Eq. (A6) into Eq. (A2), we obtain the nonadiabatic response of electrons,

$$\phi_1 = \left[\frac{T_{e0}}{e} + i\frac{\nu_{ei}k_y m_e\Delta u_0}{ek_z^2}(u_{e0} - u_{i0})\right]\frac{n_{i1}}{n_{i0}}, \tag{A7}$$

which is Eq. (29). This nonadiabatic response only modifies one element of the Hamiltonian matrix H, i.e., the (3,1) element. For Eq. (A3), the nonadiabatic part of ϕ_1, i.e., the second term on the right-hand side of Eq. (A7) cancels with the collision term, and the perturbed parallel momentum equation for ions remains the same as the collisionless case. After normalization using the scheme listed in Eqs. (13)–(15), we obtain the Hamiltonian matrix H_ν given by Eq. (30).

[1] L. I. Rudakov and R. Sagdeev, Soviet Phys. JETP **10**, 952 (1960).
[2] N. A. Krall and M. N. Rosenbluth, Phys. Fluids **6**, 254 (1963).
[3] W. Tang, Nucl. Fusion **18**, 1089 (1978).
[4] W. Horton, Rev. Mod. Phys. **71**, 735 (1999).
[5] W. Horton, *Turbulent Transport in Magnetized Plasmas* (World Scientific, Singapore, 2017).
[6] M. N. Rosenbluth and F. L. Hinton, Phys. Rev. Lett. **80**, 724 (1998).
[7] B. Coppi, Phys. Fluids **10**, 582 (1967).
[8] S. E. Parker, W. W. Lee, and R. A. Santoro, Phys. Rev. Lett. **71**, 2042 (1993).
[9] N. A. Krall and M. N. Rosenbluth, Phys. Fluids **8**, 1488 (1965).
[10] M. Landreman, T. M. Antonsen, and W. Dorland, Phys. Rev. Lett. **114**, 095003 (2015).
[11] W. Dorland, F. Jenko, M. Kotschenreuther, and B. N. Rogers, Phys. Rev. Lett. **85**, 5579 (2000).
[12] F. Jenko, W. Dorland, M. Kotschenreuther, and B. N. Rogers, Phys. Plasmas **7**, 1904 (2000).
[13] A. Dimits, W. Nevins, D. Shumaker, G. Hammett, T. Dannert, F. Jenko, M. Pueschel, W. Dorland, S. Cowley, J. Leboeuf, T. Rhodes, J. Candy, and C. Estrada-Mila, Nucl. Fusion **47**, 817 (2007).
[14] H. W. Hendel, Phys. Fluids **11**, 2426 (1968).
[15] F. L. Hinton and C. W. Horton, Phys. Fluids **14**, 116 (1971).
[16] L. Chen, P. Guzdar, J. Hsu, P. Kaw, C. Oberman, and R. White, Nucl. Fusion **19**, 373 (1979).
[17] B. Kadomtsev and O. Pogutse, Nucl. Fusion **11**, 67 (1971).
[18] C. S. Liu, M. N. Rosenbluth, and W. M. Tang, Phys. Fluids **19**, 1040 (1976).
[19] M. Kotschenreuther, W. Dorland, M. A. Beer, and G. W. Hammett, Phys. Plasmas **2**, 2381 (1995).
[20] W. W. Lee, Phys. Fluids **26**, 556 (1983).
[21] S. E. Parker, C. Kim, and Y. Chen, Phys. Plasmas **6**, 1709 (1999).
[22] A. M. Dimits, G. Bateman, M. A. Beer, B. I. Cohen, W. Dorland, G. W. Hammett, C. Kim, J. E. Kinsey, M. Kotschenreuther, A. H. Kritz, L. L. Lao, J. Mandrekas, W. M. Nevins, S. E. Parker, A. J. Redd, D. E. Shumaker, R. Sydora, and J. Weiland, Phys. Plasmas **7**, 969 (2000).
[23] G. W. Hammett and F. W. Perkins, Phys. Rev. Lett. **64**, 3019 (1990).
[24] W. Dorland and G. W. Hammett, Phys. Fluids B **5**, 812 (1993).
[25] G. W. Hammett, M. A. Beer, W. Dorland, S. C. Cowley, and S. A. Smith, Plasma Phys. Control. Fusion **35**, 973 (1993).
[26] P. A. M. Dirac, Proc. R. Soc. Lond. Ser. A: Math. Phys. Sci. **180**, 1 (1942).
[27] W. Pauli, Rev. Mod. Phys. **15**, 175 (1943).
[28] T. Lee and G. Wick, Nucl. Phys. B **9**, 209 (1969).
[29] C. M. Bender and S. Boettcher, Phys. Rev. Lett. **80**, 5243 (1998).
[30] C. M. Bender, D. C. Brody, and H. F. Jones, Phys. Rev. Lett. **89**, 270401 (2002).
[31] C. M. Bender, Rep. Prog. Phys. **70**, 947 (2007).
[32] C. M. Bender and P. D. Mannheim, Phys. Lett. A **374**, 1616 (2010).
[33] A. Mostafazadeh, J. Math. Phys. **43**, 205 (2002).
[34] A. Mostafazadeh, J. Math. Phys. **43**, 2814 (2002).
[35] A. Mostafazadeh, J. Math. Phys. **43**, 3944 (2002).
[36] R. Zhang, H. Qin, and J. Xiao, J. Math. Phys. **61**, 012101 (2020).
[37] H. Qin, R. Zhang, A. S. Glasser, and J. Xiao, Phys. Plasmas **26**, 032102 (2019).
[38] Y. Fu and H. Qin, New J. Phys. **22**, 083040 (2020).
[39] M. Krein, Doklady Akad. Nauk. SSSR N.S. **73**, 445 (1950).
[40] I. M. Gel'fand and V. B. Lidskii, Uspekhi Mat. Nauk **10**, 3 (1955).
[41] V. Yakubovich and V. Starzhinskii, *Linear Differential Equations with Periodic Coefficients*, Vol. I (Wiley, New York, 1975).
[42] O. N. Kirillov, *Nonconservative Stability Problems of Modern Physics*, Studies in Mathematical Physics Vol. 14 (Walter de Gruyter, Berlin, 2013).
[43] J. B. Parker, J. B. Marston, S. M. Tobias, and Z. Zhu, Phys. Rev. Lett. **124**, 195001 (2020).
[44] C. M. Bender (private communication, 2019).
[45] R. Zhang, H. Qin, R. C. Davidson, J. Liu, and J. Xiao, Phys. Plasmas **23**, 072111 (2016).
[46] H. Qin, J. Math. Phys. **60**, 022901 (2019).
[47] H. Qin, R. C. Davidson, J. W. Burby, and M. Chung, Phys. Rev. Spec. Top.–Accel. Beams **17**, 044001 (2014).
[48] H. Qin, M. Chung, R. C. Davidson, and J. W. Burby, Phys. Plasmas **22**, 056702 (2015).
[49] M. Chung, H. Qin, L. Groening, R. C. Davidson, and C. Xiao, Phys. Plasmas **22**, 013109 (2015).
[50] A. E. Fraser, M. J. Pueschel, P. W. Terry, and E. G. Zweibel, Phys. Plasmas **25**, 122303 (2018).
[51] A. K. Sen, J. Chen, and M. Mauel, Phys. Rev. Lett. **66**, 429 (1991).
[52] L. Schmitz, D. P. Fulton, E. Ruskov, C. Lau, B. H. Deng, T. Tajima, M. W. Binderbauer, I. Holod, Z. Lin, H. Gota, M. Tuszewski, S. A. Dettrick, and L. C. Steinhauer, Nat. Commun. **7**, 13860 (2016).